

PPPL-2045

UCSD-F,G

① I 12392

PPPL-2045

Dr. 1966-6

PPPL--2045


DE84 003466

SURVEY OF ATOMIC PROCESSES IN EDGE PLASMAS

By

R.K. Janev, D.E. Post, W.D. Langer, K. Evans,
D.B. Heifetz, and J.C. Weisheit

NOVEMBER 1983

PLASMA
PHYSICS
LABORATORY 

PRINCETON UNIVERSITY
PRINCETON, NEW JERSEY

PREPARED FOR THE U.S. DEPARTMENT OF ENERGY,
UNDER CONTRACT DE-AC82-76-CO-3073.

DISTRIBUTION OF THIS DOCUMENT IS UNLIMITED

UNCLASSIFIED

SURVEY OF ATOMIC PROCESSES IN EDGE PLASMAS

R. K. Janev[†], D. E. Post, W. D. Langer, K. Evans^{††}

D. B. Heifetz, and J. C. Weisheit[§]

Plasma Physics Laboratory, Princeton University

Princeton, New Jersey 08544

MASTER

ABSTRACT

A review of the most important reactions of atomic and molecular hydrogen with the fusion edge plasma electrons and ions is presented. An appropriate characterization of the considered collision processes, useful in plasma edge studies (evaluated cross sections, reaction rates, energy gain/loss per collision, etc.) has been performed. While a complete survey of atomic physics of fusion edge plasmas will be given elsewhere shortly, we demonstrate here the relevance of the atomic collision processes for describing the physical state of edge plasmas and understanding the energy balance in cool divertor plasmas. It is found that the excited neutral species play an important role in the low-temperature, high-density plasmas.

DISCLAIMER

This report was prepared as an account of work sponsored by an agency of the United States Government. Neither the United States Government nor any agency thereof, nor any of their employees, makes any warranty, express or implied, or assumes any legal liability or responsibility for the accuracy, completeness, or usefulness of any information, apparatus, product, or process disclosed, or represents that its use would not infringe privately owned rights. Reference herein to any specific commercial product, process, or service by trade name, trademark, manufacturer, or otherwise does not necessarily constitute or imply its endorsement, recommendation, or favoring by the United States Government or any agency thereof. The views and opinions of authors expressed herein do not necessarily state or reflect those of the United States Government or any agency thereof.

[†]Permanent address: Institute of Physics, Belgrade, Yugoslavia.

^{††}Permanent address: Argonne National Laboratory, Argonne, IL.

[§]Permanent address: Lawrence Livermore National Laboratory, Livermore, CA.

DISTRIBUTION OF THIS DOCUMENT IS UNLIMITED

124

I. INTRODUCTION

Atomic processes play a very important role in determining the behavior of edge plasmas. McNeil¹ and Terry² have pointed out the importance of molecular effects in edge plasmas. Ionization, charge exchange, excitation and radiative decay, and dissociation all influence the particle and energy balance at the edge. The temperatures that characterize the edge plasma (1-50 eV) are lower than the temperatures associated with the central plasma. While there exist many reasonable data bases for collisional processes at high temperatures,^{3,4} until recently, little attention has been paid to collisions at low temperatures.⁵ We have begun a systematic study of all the possible reactions to assess their relative importance in plasmas with $1 \text{ eV} < T_e < 50 \text{ eV}$ and $10^{12} < n_e < 10^{15} \text{ cm}^{-3}$. There are thirty or more different collisional processes that are of potential importance for H and H₂ in cool plasmas, and another twenty or so for He in a H⁺ plasma. A full account of edge plasma atomic processes along with a relatively complete characterization (cross section, reaction rate coefficients, energy loss/gain per collision, etc.) will appear in a later paper. The data are obviously too voluminous for a short paper. Therefore, we shall list here only a few of these reactions (with their maximum cross sections), give two examples of applications, and point out where the new data might be expected to have an impact on our picture of the behavior of edge plasmas.

One of the main purposes of our survey has been to upgrade the atomic physics in our divertor codes,⁶ which already include about 20 reactions. The first application is a characterization of the role of excited states of hydrogen through multiple collisions. A second application is a discussion of the possible role of molecular dissociation in the energy balance of edge plasmas.

II. COLLISIONS

A. Atomic hydrogen

Atomic hydrogen can either be excited or ionized by electron impact collisions. Table I lists a few of the typical reactions, with the corresponding maximum values of the cross sections, (σ_{\max}), the energies at which these maxima appear and the electron energy loss ΔE for each reaction. We have put together scalings for all of the relevant transitions including excitation from the groundstate to different excited states, excitation and deexcitation between levels, radiative decay and ionization. Those rates are necessary for the computation of hydrogen radiation losses and ionization and recombination rates.

TABLE I. Atomic Hydrogen

	$\sigma_{\max}(\text{cm}^2)$	$E(\sigma_{\max})$ eV	$\Delta E(\text{eV})$
$e^- + \text{H}(1s) + e^- + \text{H}(2s)$	2×10^{-17}	10	10.2
$e^- + \text{H}(1s) + e^- + \text{H}(2p)$	8×10^{-17}	50	10.2
$e^- + \text{H}(1s) + 2e^- + \text{H}^+$	7×10^{-17}	20	13.6
$e^- + \text{H}(2s) + 2e^- + \text{H}^+$	8×10^{-16}	20	3.4

B. Molecular hydrogen excitation

Molecular hydrogen is formed at the walls from recycling plasma and is introduced as gas. The excitation of molecular hydrogen can be a source of radiation. The relevant excitations are listed in Table II, and the energy levels and states are shown in Fig. 1 (taken from Sharpe⁷). Table II lists

the maximum cross section, the electron energy at the maximum, and the average electron energy loss during the collisions. The excitations to the B and C states are the dominant reactions. Due to the variety of vibrational levels available, the radiation appears as bands.

TABLE II. Molecular Hydrogen Excitations

	$\sigma_{\max}(\text{cm}^2)$	$E(J_{\max})$	E_{loss}
$e^- + \text{H}_2(v=0) + e^- + \text{H}_2(v=1)$	5×10^{-17}	2.3 eV	0.5 eV
$e^- + \text{H}_2(v=0) + e^- + \text{H}_2(v=2)$	9×10^{-17}	5 eV	1.0 eV
$e^- + \text{H}_2(X) + e^- + \text{H}_2(B)$	4×10^{-17}	70 eV	12.1 eV
(Lyman Band)			
$e^- + \text{H}_2(X) + e^- + \text{H}_2(C)$	4×10^{-17}	50 eV	12.4 eV
(Werner Band)			
$e^- + \text{H}_2(X) + e^- + \text{H}_2(E, F)$	5×10^{-18}	70 eV	12.7 eV

C. Molecular hydrogen dissociation

There are four principal reactions. These are listed in Table III, (see also Fig. 1) with their maximum cross sections, electron impact energy at maximum, average electron energy loss in the collision, and the average kinetic energy of the dissociated atoms. The cross sections for dissociating vibrationally excited H_2 are expected to be significantly larger than the groundstate cross sections, particularly for the first reaction in Table III, since the threshold would be reduced significantly, and the "size" of the molecule becomes larger as the vibrational quantum number v increases.

D. Molecular ionization

The rate coefficient is given in Freeman and Jones,³ and the electron energy loss is 15.4 eV.

E. Dissociative ionization of H₂

The reaction $e^- + H_2 \rightarrow e + H^+ + H(1s)$ proceeds through various excited states of H_2^+ (see Fig. 1) and has a threshold of 16-18 eV. The maximum cross section for $e^- + H_2(X)$ (the groundstate) is 6×10^{-18} and it peaks at 120 eV. The electron energy loss can vary from 18 eV to 38 eV depending on the incident energy which affects the dissociative channel that can be attained. The energy of each of the products varies between 0 and 7.8 eV.

TABLE III. Molecular Dissociation

	$\sigma_{\max}(\text{cm}^2)$	$E(\sigma_{\max})$	E_{loss}	$\bar{E}(H_0)$
$e^- + H_2(X) \rightarrow e^- + H(1s) + H(1s)$	9×10^{-17}	20 eV	10.5 eV	3 eV
$e^- + H_2(X) \rightarrow e^- + H(1s) + H^*(2s)$	1.7×10^{-17}	50 eV	15.3 eV	0.3 eV
$e^- + H_2(X) \rightarrow e^- + H^*(2p) + H^*(2s)$	0.3×10^{-17}	60 eV	34.6	4.85 eV
$e^- + H_2(X) \rightarrow e^- + H(1s) + H^*(n=3)$	0.2×10^{-17}	50 eV	21.5	2.5 eV

F. Dissociation of H_2^+ and negative ion formation

H_2^+ is primarily produced from ionization of H₂ by electron impact. Examination of the potential energy diagram shows that the Franck-Condon transitions from H₂(v=0) to H_2^+ leave the H_2^+ vibrationally excited. A few sample H_2^+ reactions are listed in Table IV. The major item to note is that

the cross section for vibrationally excited $H_2(v) + e + H^+ + H^O + 2e^-$ is very large, much larger than the fits in Jones,⁴ as has been pointed out by Harrison.⁵

TABLE IV. Molecular Ion Collisions and Negative Ions

	σ_{max}	$E(\sigma_{max})$	ΔE_e	$E(H^+ \text{ or } H)$
$e^- + H_2^+(v) + 2e^- + 2H^+$ $v=0-7$	$1.7 \times 10^{-17} \text{ cm}^2$	100 eV	15.5 eV	0.4 eV
$e^- + H_2^+(v) + 2e^- + H^+ + H(1s)$	10^{-15} cm^2	4 eV	10.5 eV	4.3 eV
$e^- + H_2^+(v) + 2e^- + H^+ + H(n=2)$	$(4 \times 10^{-17} \text{ cm}^2)$	35 eV	12.5 eV	2.5 eV
$e^- + H_2^+(v) + H^O(1s) + H(n)$	$(4 \times 10^{-18} \text{ cm}^2 \text{ at } 10 \text{ eV})$	E_e	$\frac{1}{2} (E_e - \frac{13.6}{n^2})$	
$e^- + H_2(v > 4) + H^- + H$	$(6 \times 10^{-16} \text{ cm}^2 \text{ at } 1 \text{ eV})$	$\lesssim 0.75 \text{ eV}$	$\frac{1}{2} E_e$	

At very low energies H^- can be formed due to the large cross sections for electron attachment to vibrationally excited H_2 . Since $H^+ + H^- + 2H_0$ is extremely rapid, the volume recombination rate could be extremely large for such a cold plasma ($T_e \lesssim 2 \text{ eV}$) provided that appreciable amounts of vibrationally excited H_2 are present.

G. A few relevant heavy particle collisions

Table V lists several relevant heavy particle collisions. The first reaction has a large cross section and indicates that appreciable amounts of vibrationally excited H_2 could be produced by proton collisions. The second reaction has the same effect. Since almost all of the H_2^+ produced is

vibrationally excited, the large charge-exchange cross section implies that a large amount of vibrationally excited H_2 could also be present.

TABLE V. Heavy Particle Collisions

	σ_{\max}	$E(\sigma_{\max})$
$p + H_2(v=0) \rightarrow p + H_2(v>0)$	10^{-15}cm^2	15 eV
$H_2^+ + H_2(v') \rightarrow H_2(v) + H_2^+(v')$	10^{-15}cm^2	$1-10^4$ eV

III. CHARACTERIZATION OF MULTISTEP PROCESSES INVOLVING ATOMIC HYDROGEN

Recycling at the plasma edge is partially determined by the ionization rate of neutral hydrogen atoms and molecules. Thus accurate data on the ionization and recombination rates of hydrogen atoms and ions are quite useful. In addition, hydrogen line radiation can be an important energy loss mechanism. The measurements of hydrogen light are a key diagnostic tool for interpreting particle recycling. These processes occur in the 2-100 eV temperature and $10^{12}-10^{15} \text{cm}^{-3}$ density range. At such densities and temperatures, the usual coronal approximation may not be valid in that the electron collision time may be shorter than the radiative decay time for highly excited atoms. Thus one often needs to consider a "collisional-radiative" treatment of the problem including excited states, collisional excitation and deexcitation, radiative decay and collisional ionization.^{8,9} We have done such a calculation using a prescription following Weisheit.¹⁰ The basic result is that at high densities, the ionization and recombination rates are increased due to multistep collisions. The atom can first be

excited from $n=1$ to a higher state n . Then it can be more easily ionized from the excited level n since the electron binding energy is smaller. The ionization rates and charge-exchange rates both increase roughly as n^2 . The excitation rate from the groundstate to a state with a principle quantum number n decreases roughly as $1/n^3$, but the lifetime increases roughly as n^3 , so there can be an appreciable fraction of the atoms in Rydberg states. As the density increases, three-body recombination, followed by collisional deexcitation can also become important. In practice, the upper n is limited by Lorentz ionization. For hydrogen, the upper n is given roughly by $n_c = 39 / (B(T) \sin \theta \sqrt{E(\text{eV})/A})^{1/4}$ where n_c is the principal quantum number of the highest bound level, B is the field in Tesla, θ is the angle between the particle trajectory and the field, A is the atomic number of the atom, and E is the kinetic energy of the atom in eV. For typical conditions, ($B(T) \sim 2T$, $\sin \theta \sim 0.5$, $E \sim 10$ eV, $A = 1$), $n_c = 26$. We have taken about this number of levels into account in our calculations.

Figure 2 shows the electron ionization rate for a family of densities from 10^{15}cm^{-3} . Also shown is the commonly used fit from Freeman and Jones.³ As expected, the ionization rate increases with density for a fixed energy. In extreme cases the rate may be increased up to an order of magnitude or more by multistep processes.

Figure 3 shows the recombination rate as a function of T_e , again for a family of densities. For comparison a commonly used calculation by Gordeev et al.¹¹ is shown. The rate at low T_e ($\sim 1-10$ eV) can be significantly higher than the groundstate value. However, this result is probably not useful since the rate is still too small to affect edge plasmas significantly. Recombination takes place primarily when the plasma hits the wall. Part of the increase in the recombination rate is due to three-body recombination

effects, which are not reflected in the radiative recombination calculation of Gordeev et al.

Energy losses due to radiation from radiative decay can be significant.

Figure 4 shows the energy per ionization radiated:

$$\left[\sum_{n>m} \alpha(n \rightarrow m) \Delta E_{nm} + \sum_n \langle \sigma_{n \rightarrow \infty} v \rangle 13.6 \text{ eV} \right] / \sum_n \langle \sigma_{n \rightarrow \infty} v \rangle,$$

where the sum over all the levels $n, \alpha(n \rightarrow m)$ is the radiative decay rate from n to m , ΔE_{nm} is the energy difference between levels n and m , and $\sigma_{n \rightarrow \infty}$ is the ionization cross section of level n . The typical value used by plasma modelers is ~ 40 eV which is a pretty good estimate for $T_e \gtrsim 50$ eV and $n \lesssim 10^{13} \text{ cm}^{-3}$. At higher densities the multistep processes interfere with the radiative losses, by ionizing the excited states before they can radiatively decay.

For electrons with energies much greater than 13.6 eV ($T \gtrsim 15$ eV), there is little difference (at most, a factor of 2) between the electron excitation and ionization rates. Thus multistep processes involving excited states are relatively unimportant. Electrons with energies between 10.2 eV (the excitation energy of $n=2$ level) and 13.6 eV (the groundstate ionization potential) can excite or ionize only the states with $n > 2$. The ratio f_e ($10.2 < E < 13.6$ eV) / $f_e(E > 13.6$ eV) can become very large at low temperatures, and one can have many excitations per ionization. Once an electron gets excited to the $n=2$ level, then the transition to $n=3$ takes 1.89 eV and to $n=\infty$ takes 3.4 eV. For $T_e \sim 1-5$ eV there are plenty of electrons with those energies. Thus, we expect the biggest effects to occur when $T_e \lesssim 5-6$ eV, which is where the increases in the ionization and radiation rates become large (see Fig. 4).

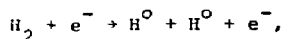
We use these rates in our neutral gas transport calculations.⁶ The code also computes the H_{α} , etc. radiation which is useful for comparing with the commonly used H_{α} diagnostics.

One might speculate that a similar calculation would be necessary to determine the molecular radiation, and ionization and recombination. However, the lifetimes of the excited states of H_2 are all very short; thus the assumption that all H_2 molecules are in the ground electronic state is acceptable.

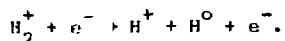
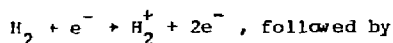
IV. POSSIBLE ROLE OF MOLECULES IN THE ENERGY BALANCE OF COOL PLASMAS

Recent bolometer measurements on PDX diverted discharges and thermocouple measurements of the power loading on the divertor neutralizer plates show that less than 20-30% of the heating power in ohmic and beam heated discharges hit the neutralizer plates in the divertor or is measured by the bolometers as fast neutrals or radiation. In ohmic discharges, the heating power is of the order of 300-500 kW, while in beam heated discharges the power may be as high as 5-6 MW. We discuss the possibility that the dissociation of hydrogen molecules can account for the missing power.

The relevant reactions are



and



The first reaction has a $\langle \sigma v \rangle$ of about $10^{-8} \text{ cm}^3/\text{sec}$ for $v=0$, and for higher v , the rate is greater. The electron loses $\sim 10 \text{ eV}$ in the collision and the H_0 atoms carry off about 3 eV each. As we have seen in Sec. II, vibrationally excited H_2 could be present in reasonable quantities due to $p + \text{H}_2$ collisions and $\text{H}_2^+ + \text{H}_2$ charge exchange. The second chain of reactions has rates of $\sim 10^{-8} \text{ cm}^3/\text{sec}$ at $T_e \sim 10 \text{ eV}$. The electron loses about 15 eV in the ionization. The rate for the second reaction (dissociation of H_2^+) is $10^{-7} \text{ cm}^3/\text{sec}$ for groundstate H_2^+ and larger for vibrationally excited H_2^+ . The electron energy loss in this case is about 10 eV , and the reaction products have energies of $\sim 4 \text{ eV}$. The picture is summarized in Table VI.

The H_2^+ thus formed will have a good chance to equilibrate thermally due to Coulomb collisions in the scrape-off plasma, thus cooling the scrapeoff. In addition, the proton from the $\text{H}_2 + e^- + \text{H} + \text{H}^+ + e^-$ will further cool the plasma.

TABLE VI. Molecular Dissociation

	Rate	ΔE	$2E(\text{H}^0)$
$\text{H}_2 + e \rightarrow 2\text{H}^0$	$> 10^{-8} \text{ cm}^3/\text{sec}$	10 eV	6 eV
$\text{H}_2 + e^- + \text{H}_2^+ \rightarrow \text{H}^0 + \text{H}^+$	$> 10^{-8} \text{ cm}^3/\text{sec}$	25 eV	$4 \text{ eV H}^0 + 4 \text{ eV H}^+$

We now analyze whether rates of $10^{-8} \text{ cm}^3/\text{sec}$ or greater, and energy losses of $10\text{-}25 \text{ eV}$ can account for much of the heating power in the PDX divertor given the measured pressures, temperatures, and densities. A further consideration is that fast H^0 's are not observed to reach the bolometer, so

they must scatter before reaching the bolometer.

Using the measurements of elastic scattering at 1 eV and extrapolating to higher energies, σ for $H + H_2$ is $\sim 10^{-15} \text{cm}^2$.¹² The PDX diverted plasma is roughly 35 cm high. The measured line densities vary from $10^{13}/\text{cm}^2$ to $6 \times 10^{13}/\text{cm}^2$.¹³ The neutral density varies from $8.4 \times 10^{12} \text{cm}^{-3}$ to $4.2 \times 10^{13} \text{cm}^{-3}$ as measured by ionization gauges about 100 cm from the neutralizer plate. The actual molecular density near the neutralizer plate may be significantly higher. The power loss rate is then

$$P = \int n_e n_{H_2} (\Sigma \langle \sigma v \rangle \Delta E) dv,$$

where $\Sigma \langle \sigma v \rangle \Delta E \sim q 10^{-8} (10 \text{ eV} + 25 \text{ eV})$. Due to the effects of vibrational excitation, q is probably larger than 1. Letting the line density be $n \times 10^{13}$ and the neutral density be $m \times 8.4 \times 10^{12}/\text{cm}^3$, we obtain for a major radius of 100 cm and two neutralizer plates, $P = nmq \times 10^5 \text{ W}$. Since n is observed over the range 1 to 6, and m varies from 2 to 10, and q can be larger than 1 (maybe as large as 5), molecular dissociation can account for powers from 200 kW up to 5 MW or more.

The picture of energy loss in the divertor then is that the molecules form at the divertor chamber walls, dissociate in the diverted plasma carrying away at least 12 eV of energy (kinetic plus binding) and maybe as much as 25 eV if the proton from H_2^+ dissociation recombines into an excited state at the surface. The atoms then elastically scatter with the molecules in the chamber, producing a hot gas which is relatively isotropic. The gas cools in the bolometer tube, so the energy does not reach the bolometer. For an H_2 density of $2 \times 10^{13} \text{cm}^{-3}$, $\lambda = 1/n\sigma \sim 50 \text{ cm}$, and the fast neutrals would be scattered, since the distance to the bolometer is $\sim 100 \text{ cm}$.

In addition, much of the dissociation could take place in the divertor throat, where the bolometer cannot detect the emission. The fast atoms thus formed could be sprayed around the main chamber, liners, and divertor domes.

V. SUMMARY

In past models,⁶ a large number (~ 20) of atomic reactions were taken into account. However, at temperatures of 10 eV or less, densities in the $10^{13}/\text{cm}^3$ range, and in the presence of high H_2 pressures, even more complicated atomic and molecular effects than previously considered can become quite important. We have begun a systematic survey of the possible important reactions, and have discussed a few in this paper. We applied some of these data to several relevant problems. While the collisional radiative problem for hydrogen has been studied before by several groups, we have repeated the calculation and systemized the results for plasma applications.

We have also examined, albeit somewhat qualitatively, the possibility that molecular dissociation could be the dominant plasma edge cooling mechanism in a high recycling divertor.

Among the new features of our presentation of data is the role of vibrationally excited H_2 and H_2^+ . In particular, vibrationally excited H_2 and H_2^+ are easier to dissociate than groundstate configurations, and vibrationally excited H_2 may be present in larger amounts than we previously thought.

Vibrationally excited H_2 also opens the possibility of an efficient volume recombination mechanism if $T \lesssim 2-4$ eV, through the reaction chain $\text{H}_2(v=0) + \text{H}_2^+(v')$ \rightarrow $\text{H}_2^+(v=0) + \text{H}_2^0(v')$, $\text{H}_2^0(v') + e^- \rightarrow \text{H}^- + \text{H}^0$, and $\text{H}^- + \text{H}^+ \rightarrow 2\text{H}^0$. This would be the first identification of a recombination mechanism that would make possible the widely proposed "gaseous neutralizer" divertors.

ACKNOWLEDGMENT

This work was supported by the U.S. Department of Energy Contract No. DE-AC02-76-CHO-3073.

REFERENCES

- ¹D. McNeil and J. Kim, Phys. Rev. A 25, 2152 (1982).
- ²J. Terry, MIT Plasma Fusion Center Report No. PFC/JA 82-3, 1982.
- ³R. Freeman and E. Jones, Culham Laboratory Report No. CLM-R-137, 1974.
- ⁴E. M. Jones, Culham Laboratory Laboratory Report No. CLM-R-175, 1977.
- ⁵M. Harrison, in Atomic and Molecular Processes in Controlled Thermonuclear Fusion, edited by C. Joachain and D. Post (Plenum, New York, 1983).
- ⁶D. Heifetz, D. Post, M. Petravic, J. Weisheit, and G. Bateman, J. Comput. Phys. 42, 309 (1982).
- ⁷T. Sharp, At. Data Nucl. Data Tables 2, 120 (1972).
- ⁸D. R. Bates, A. Kingston, and R. McWhirter, Proc. Roy. Soc. London, Ser. A: A267, 297 (1962).
- ⁹R. P. McWhirter and A. Hearn, Proc. Phys. Soc. London 92, 641 (1963).
- ¹⁰J. Weisheit, J. Phys. B: 8, 2556 (1975).
- ¹¹Yu. Gordeev et al., Pis'ma Zh. Eksp. Teor. Fiz. [JETP Lett.] 25, 223 (1977).
- ¹²"Cross Sections for Atomic Processes," edited by Takayanagi and Suzuki, (University of Nagoya, Nagoya, Japan, 1978) Vol. 1.
- ¹³M. G. Bell et al., "The Energy Balance of Divertor Discharges in the PDX Tokamak," presented at the Symposium on Energy Removal and Particle Control in Toroidal Fusion Devices, Princeton Plasma Physics Laboratory, Princeton, NJ, July 1983 (in press).

FIGURE CAPTIONS

- FIG. 1. Potential energy curves for H_2 for the levels appropriate for molecular excitation.
- FIG. 2. The electron ionization rate as a function of the electron temperature for a family of densities. The value of Freeman and Jones is also given.³
- FIG. 3. Radiative recombination rate ($H^+ + e \rightarrow H^0$) as a function of electron temperature for a family of electron densities. The value of Gordeev is also given.¹¹
- FIG. 4. The ratio of the radiation loss rate plus the product of the ionization rate and the ionization potential to the ionization rate as a function of T_e for a family of densities.

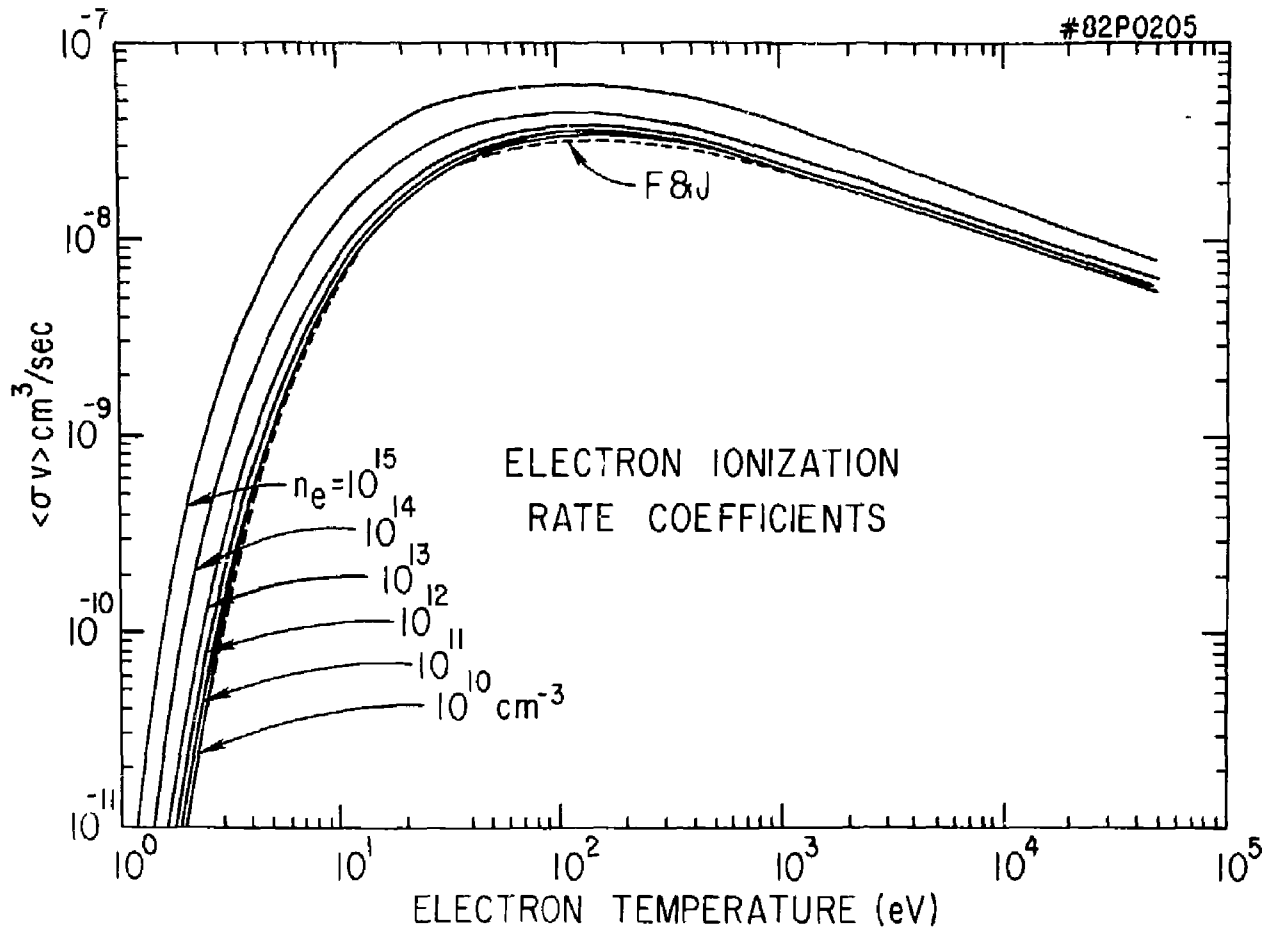


FIG. 2

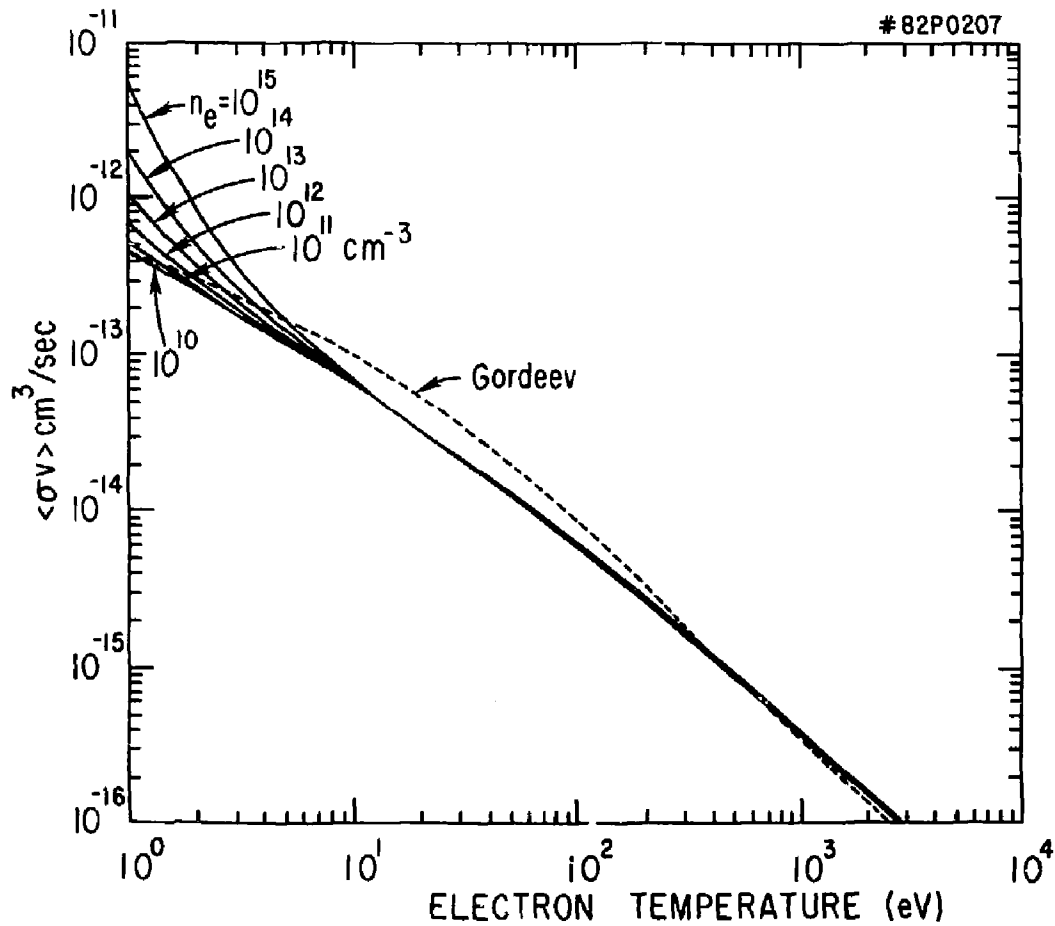


FIG. 3

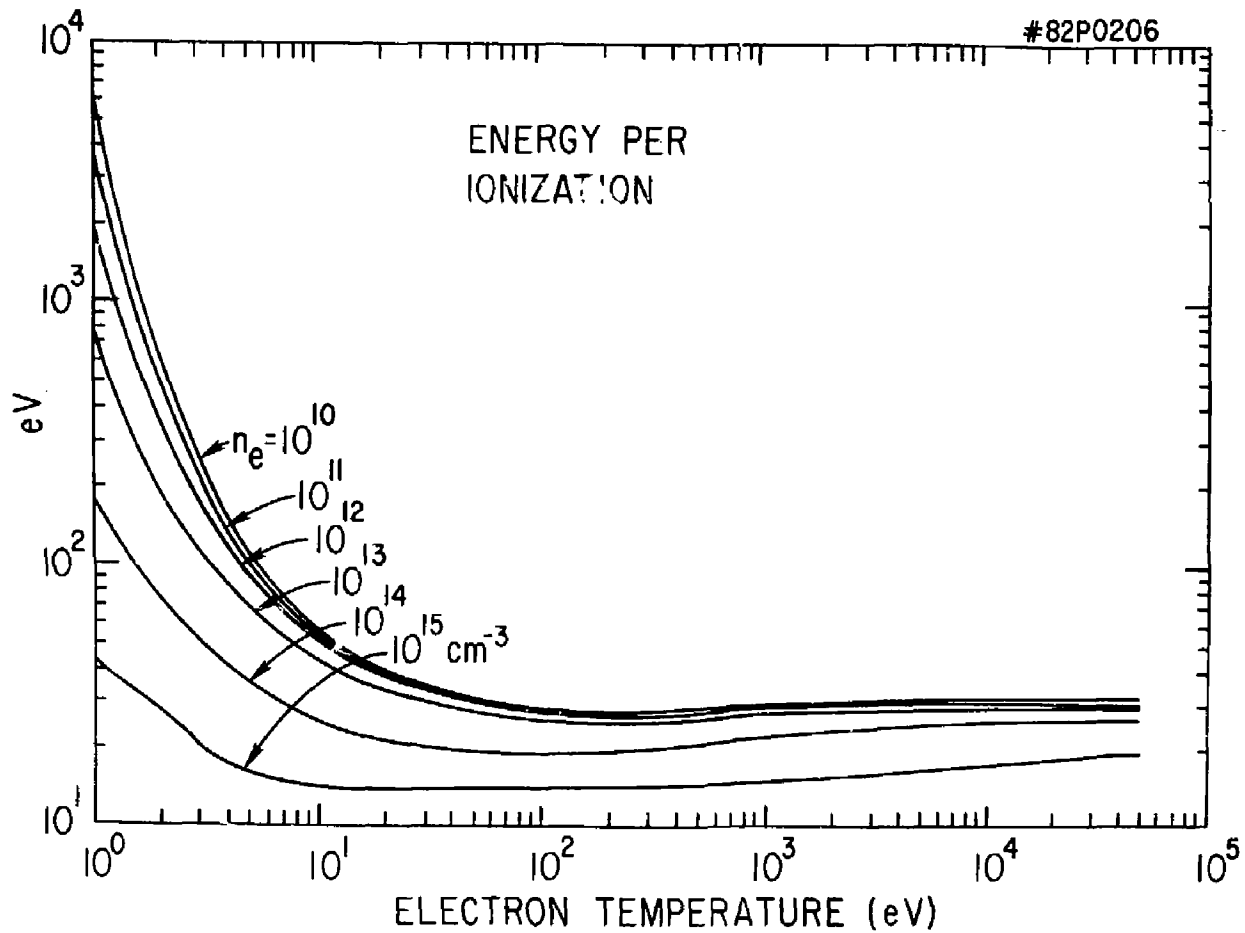


FIG. 4

EXTERNAL DISTRIBUTION IN ADDITION TO TIC UC-20

Plasma Res Lab, Austra Nat'l Univ, AUSTRALIA
 Dr. Frank J. Paoloni, Univ of Wollongong, AUSTRALIA
 Prof. I.R. Jones, Flinders Univ., AUSTRALIA
 Prof. M.H. Brennan, Univ Sydney, AUSTRALIA
 Prof. F. Cap, Inst Theo Phys, AUSTRIA
 Prof. Frank Verheest, Inst theoretische, BELGIUM
 Dr. D. Palumbo, Dg XII Fusion Prog, BELGIUM
 Ecole Royale Militaire, Lab de Phys Plasmas, BELGIUM
 Dr. P.H. Sakanaka, Univ Estadual, BRAZIL
 Dr. C.R. James, Univ of Alberta, CANADA
 Prof. J. Teichmann, Univ of Montreal, CANADA
 Dr. H.M. Skarsgard, Univ of Saskatchewan, CANADA
 Prof. S.R. Sreenivasan, University of Calgary, CANADA
 Prof. Tudor W. Johnston, INRS-Energie, CANADA
 Dr. Hannes Bernard, Univ British Columbia, CANADA
 Dr. M.P. Bachynski, MPB Technologies, inc., CANADA
 Zhengou Li, SW Inst Physlcs, CHINA
 Library, Tsing Hua University, CHINA
 Librarian, Institute of Physics, CHINA
 Inst Plasma Phys, Academia Sinica, CHINA
 Dr. Peter Lukac, Komenskeho Univ, CZECHOSLOVAKIA
 The Librarian, Culham Laboratory, ENGLAND
 Prof. Schetzman, Observatoire de Nice, FRANCE
 J. Radet, CEN-BP6, FRANCE
 AM Dupas Library, AM Dupas Library, FRANCE
 Dr. Tom Mual, Academy Bibliographic, HONG KONG
 Preprint Library, Cent Res Inst Phys, HUNGARY
 Dr. S.K. Trehan, Panjab University, INDIA
 Dr. Indra, Mohan Lal Das, Banaras Hindu Univ, INDIA
 Dr. L.K. Chevda, South Gujarat Univ, INDIA
 Dr. R.K. Chhajlani, Var Ruchi Marg, INDIA
 P. Kaw, Physical Research Lab, INDIA
 Dr. Phillip Rosenau, Israel Inst Tech, ISRAEL
 Prof. S. Cuperman, Tel Aviv University, ISRAEL
 Prof. G. Rostagni, Univ DI Padova, ITALY
 Librarian, Int'l Ctr Theo Phys, ITALY
 Miss Ciella De Palo, Assoc EURATOM-CNEN, ITALY
 Biblioteca, del CNR EURATOM, ITALY
 Dr. H. Yamato, Toshiba Res & Dev, JAPAN
 Prof. M. Yoshikawa, JAERI, Tokai Res Est, JAPAN
 Prof. T. Uchida, University of Tokyo, JAPAN
 Research Info Center, Nagoya University, JAPAN
 Prof. Kyoji Nishikawa, Univ of Hiroshima, JAPAN
 Prof. Sigeru Mori, JAERI, JAPAN
 Library, Kyoto University, JAPAN
 Prof. Ichiro Kawakami, Nihon Univ, JAPAN
 Prof. Satoshi Itoh, Kyushu University, JAPAN
 Tech Info Division, Korea Atomic Energy, KOREA
 Dr. R. England, Ciudad Universitaria, MEXICO
 Bibliotheek, Fom-Inst Voor Plasma, NETHERLANDS
 Prof. B.S. Lilley, University of Waikato, NEW ZEALAND
 Dr. Suresh C. Sharma, Univ of Calabar, NIGERIA
 Prof. J.A.C. Cabral, Inst Superior Tech, PORTUGAL
 Dr. Octavian Petrus, ALI CUZA University, ROMANIA
 Prof. M.A. Heilberg, University of Natal, SO AFRICA
 Dr. Johan de Villiers, Atomic Energy Bd, SO AFRICA
 Fusion Div. Library, JEN, SPAIN
 Prof. Hans Wilhelmson, Chalmers Univ Tech, SWEDEN
 Dr. Lennart Stenflo, University of UMEA, SWEDEN
 Library, Royal Inst Tech, SWEDEN
 Dr. Erik T. Karlson, Uppsala Universitet, SWEDEN
 Centre de Recherches, Ecole Polytech Fed, SWITZERLAND
 Dr. W.L. Neise, Nat'l Bur Stand, USA
 Dr. W.M. Stacey, Georg Inst Tech, USA
 Dr. S.T. Wu, Univ Alabama, USA
 Prof. Norman L. Dison, Univ S Florida, USA
 Dr. Benjamin Ma, Iowa State Univ, USA
 Prof. Magne Kristiansen, Texas Tech Univ, USA
 Dr. Raymond Askew, Auburn Univ, USA
 Dr. V.T. Tolo', Knarkov Phys Tech Ins, USSR
 Dr. D.D. Ryutov, Siberian Acad Sci, USSR
 Dr. G.A. Eliseev, Kurchatov Institute, USSR
 Dr. V.A. Glukhikh, Inst Electro-Physical, USSR
 Institute Gen. Physics, USSR
 Prof. T.J. Boyd, Univ College N Wales, WALES
 Dr. K. Schindler, Ruhr Universitat, W. GERMANY
 Nuclear Res Estab, Julich Ltd, W. GERMANY
 Librarian, Max-Planck Institut, W. GERMANY
 Dr. H.J. Kaeppeler, University Stuttgart, W. GERMANY
 Bibliothek, Inst Plasmaforschung, W. GERMANY